Heat transfer measurement techniques in microchannels for single and two-phase Taylor flow

Ayoub Abdollahi[1,*], S. Norris[1], Rajnish N. Sharma[1]

[1] Department of Mechanical Engineering, University of Auckland, 20 Symonds Street, Auckland, 1010, New Zealand

Abstract

Accurate measurement of heat transfer in experiments of single, two-phase liquid-liquid and gas-liquid Taylor flows without phase change in microchannels is a challenging task. In this paper we review experimental studies of these flows, and the methods of heat transfer measurement used, in order to gain insight into the effect of some critical dimensionless groups on the accuracy of the estimates of the heat transfer. It was found that experimental measurements of Nusselt number often disagree with theoretical predictions, particularly at low Reynolds numbers. We identify the major causes of error in experimental estimation of the Nusselt number, and propose solutions to decrease the error in experimental heat transfer measurement. Measurements obtained from a new microchannel experimental setup are reported upon, to demonstrate these sources of error.

Keywords: Single-phase flow; Taylor flow; Nusselt number; Heat transfer; Microchannel.

---

*Corresponding author:

E-mail address: Ayoubabdollahi@gmail.com (A. Abdollahi).

1 Introduction

The dissipation of high heat fluxes is an issue of increasing importance in thermal management with the continuing trend for higher performance and further miniaturisation of electronic components [1]. Based on the literature [2] traditional cooling methods are not effective enough to meet the demands of recently advanced electronic systems. Thus recent research has been focused on developing microchannel heat sinks (MCHS) as an efficacious system for heat removal from microelectronic devices.

The notion of a MCHS, described as a small mass and volume device with a large convective heat transfer coefficient together with a large surface area to volume ratio, was initially proposed in 1981 by Tuckerman and Pease [3]. The high surface to volume ratio can be achieved by passing the coolant through many small microchannels through the body to be cooled, while the high heat transfer coefficient for a MCHS is achievable by periodic disruption in the thermal boundary layer, or increased flow mixing and turbulence generation through the generation of secondary flow.

Water is the utmost desirable coolant employed in a MCHS, since water is environmental-friendly and it has a high density, thermal conductivity, and specific heat. However, the rate of heat transfer in a microchannel is significantly higher for two-phase rather than single-phase flow [1, 4]. Possible methods to achieve two-phase flow and enhance the heat transfer rate are boiling two-phase flow, and non-boiling gas-liquid or liquid-liquid systems [5].

Many published experimental studies have focused on the heat transfer behavior of both single and two-phase fluid flow in microchannels. They have studied different ranges of dimensionless numbers,

conditions, geometry and dimensions, using a range of instrumentation and measurement techniques, and provide a rich mix of data to evaluate the strengths and weaknesses of the measurement methodologies available. It is known that researchers have encountered a number of challenges in measuring bulk fluid temperature, wall temperature, and applied heat flux, in order to calculate the heat transfer rate in microchannel experiments. Some results [6, 7] are reported to be in agreement with theoretical and numerical predictions, while others [8-10] are not. These will be discussed in detail, in section 3. In addition, because of the significance of the heat transfer of single and two-phase fluid flow in microchannels, researchers have reviewed the heat transfer behaviour of single phase, boiling two-phase and non-boiling two-phase fluid flow in microchannels [5, 11]. However, the importance of the method of measuring the heat transfer rate and the accuracy of the method in microchannels has not been discussed in details.

The objectives of the current study are (1) to review the experimental heat transfer measurements in recent studies of single and two-phase fluid flows in microchannels, and determine their strengths and weaknesses; (2) to determine the parameters affecting the accuracy of heat transfer measurements by examination of new experimental and simulation data; and (3) to identify further research which needs to be undertaken in the field.

2 Dimensionless groups governing heat transfer

Many dimensionless groups or numbers have been used in the analysis of fluid flow and heat transfer. Perhaps the most significant factors representing the nature of fluid flow and heat transfer ratio are the Reynolds, Prandtl, Nusselt, and Peclet numbers.

The Reynolds number states the ratio of inertial to the viscous forces:

$$Re = \frac{\rho U D_h}{\mu} \tag{1}$$

where U, $D_h = 4A/P$, ρ and μ, are the mean fluid velocity, the hydraulic diameter of the channel, and the fluid density and dynamic viscosity, respectively. A and P are cross-sectional area and the wetted perimeter of the cross-section, respectively.

The Prandtl number defines the ratio of momentum diffusion (represented by kinematic viscosity v) to the rate of thermal diffusion (represented by thermal diffusivity α):

$$Pr = \frac{v}{\alpha} = \frac{\mu\, c_p}{k} \tag{2}$$

where k and c_p are thermal conductivity and specific heat capacity, respectively.

In common with other studies, the heat transfer rate in a microchannel is non-dimensionalised as the Nusselt number:

$$Nu = \frac{hD_h}{k} = \frac{q_w D_h}{k(T_w - T_b)} \tag{3}$$

where q_w ,T_b ,T_w and k are heat flux, bulk fluid temperature, mean inner wall temperature and thermal conductivity, correspondingly. In order to determine the local Nusselt number the local inner wall temperature along the channel, the bulk fluid temperature, and an accurate value of the wall heat flux are needed.

To find the local Nusselt number it is required to determine the local inner wall temperature and local bulk fluid temperature along the test section. Accurate and non-intrusive measurement of the inner wall temperature and bulk fluid temperature has been challenging in all experimental studies. There are a variety of techniques to measure the wall and bulk fluid temperatures and this will be discussed in the next sections.

Morini and Yang [12] and Yarin et al. [13] studied the importance of dimensionless groups on the measurement of the heat transfer rate of a microchannel. Entrance effects, viscous dissipation, conjugate wall-fluid heat transfer, axial fluid conduction, surface roughness, electro-osmotic effects and temperature-dependence of fluid properties were reported as the most important scaling effect that could affect the accurate determination of the Nusselt number. The electro-osmotic effect is important if a polar liquid is used in microchannels with silicon walls. Graetz number (Gz) is useful to predict the thermally developing flow entrance length (L). The Peclet number can be helpful to determine the importance of axial heat conduction through the fluid. Conjugate wall-fluid heat transfer is characterised by the M factor and it depends on the wall thermal conductivity k_w, the cross sectional area of heat conduction (A_c), the fluid specific heat capacity(C_p), and fluid flow rate ($\dot{m}$). Viscous dissipation is negligible if Brinkman number (Br) is lower than 0.005. Fluid properties change with varying temperature and this may need to be accounted for in calculations. Surface roughness effect is an important issue if the ratio of the roughness (e) to the diameter of the channel (D) is higher than 0.05.

It is useful to consider these dimensionless groups and their effects on microchannel heat transfer during the design of an experiment, and they are listed in Table 1. A full discretion of the scaling effects was presented by Rosa et al. [14].

Table 1 Important scaling effects affecting the Nusselt number [12-14]

Effect	Dimensionless group		Negligible if
Entrance effect	Graetz number	$Gz = RePr(\frac{D}{L})$	Gz <10
Fluid axial conduction	Peclet number	$Pe = RePr$	Pe >50
Conjugate wall-fluid heat transfer	Axial conduction number	$M = \frac{k_w A_c}{\dot{m} c_p L}$	M <0.01
Viscous dissipation	Brinkman number	$Br = \frac{\mu u^2}{q_w}$	$Br < 0.005$
Surface roughness		e/D	$\frac{e}{D} < 0.05$

3 Heat transfer measurement techniques

3.1 Local Wall temperature

Measuring the local wall temperature is essential to calculate the local heat transfer rate. There are at least two types of method to measure the local inner wall temperature of a microchannel; direct or indirect methods.

The direct method involves attaching fine high accuracy temperature measurement devices, such as resistance temperature detectors (RTDs) or thermocouples (TCs), close to the inner wall by making holes in the wall [15]. In this case a number of limitations may cause inaccuracy in the measurement of the inner wall temperature. Planting thermocouples in the holes could possibly change the temperature distribution inside the channel, or could prevent having uniform heat flux along the channel wall. This becomes more significant when the number of probes increases along the channel. Moreover, manufacturing the holes, planting the thermocouples and electrically isolating them from the heated wall can be a challenging task, particularly for a microchannel having a thin wall thickness.

To measure the local inner wall temperature by an indirect method, miniature RTDs and fine thermocouples have been the most common temperature probes used in experimental studies. In this method, thermocouples or RTDs are attached to the outer surface of the heated wall and the inner wall temperature can be estimated by assuming one-dimensional heat conduction between the outer surface and the inner wall. In order to make this assumption, it is essential to determine there is minimal axial conduction in the wall, or that the conjugate wall-fluid heat transfer M is small ($M < 0.01$) [16]. This effect becomes more significant at low mass flow rates, which for a given experiment means at low Reynolds numbers, and so typically for $Re < 100$ the temperature distribution along the microchannel

heat sink may not change linearly due to the existence of conjugate wall-fluid heat transfer. From this, the estimated value of *Nu* could be lower than the true value. This error decreases with increasing flow rate. This will be discussed in detail in section 4.

Having high accuracy miniature thermocouples may be beneficial compared to using RTDs or thermocouples with a large size relative to the channel dimensions. Miniature thermocouples smaller than the channel dimensions are able to capture the temperature at the desired points which is useful to increase the accuracy of local wall temperature measurements, while larger thermocouples measure an area-averaged temperature on the wall. Additionally, having a poor contact between a RTDs and the wall increases the errors in the measured temperature, and so it is essential to ensure a good thermal contact with the surface of the test section.

Furthermore, to increase the accuracy of measurement, it is advantageous to increase the number of probes along the microchannel. This is useful if the average wall temperature is needed for quantifying the heat losses indirectly (see section 3.3 for further discussion on this matter). RTDs may be more practical in some cases if it is necessary to electrically isolate the probes from the test section [17-19]. For example, in most experimental studies the heat flux was applied to the test section by Ohmic or Joule heating via a DC power supply and this could have been a source of noise in the temperature readings by probes, necessitating their electrical isolation. Thermocouples can be electrically isolated from the microchannel and power supply using thin highly conductive thermal tape or glue. However, the temperature reading will be wall averaged over the area of the conducting tape and the thin layer of tape may otherwise increase the error in the temperature readings and will increase the axial conduction in the microchannel wall. In some experimental studies [20], the thermocouples were glued onto the outer wall by thermally conductive silicon. There was a scatter in the experimentally determined *Nu* in comparison with the theoretical value. Using glue increases the discrepancies and this could have been a source of error in their experiment.

Soldering the thermocouples directly onto the wall can increase the accuracy of temperature measurement. However, soldering the thermocouple to the wall needs to be done carefully to prevent it becoming a hot spot which would result in an erroneous temperature reading, so it is necessary to validate the measurements to determine the quality of the joint. The thermocouples are not electrically insulated if they are soldered to the walls and so can be prone to electrical noise. Using an AC power supply can be beneficial to eliminate noise in the signals. However, it requires a complicated electrical control system to be able to supply and control a low voltage and high electric current through the microchannel. If the fluid flow is delivered to the test section by an electrical flow controller, this may interfere with temperature measurements by soldered thermocouples. Having a DC power supply as a power source for the flow controller can avoid this problem.

An optical technique is an alternative method to measure the outer wall temperature with good accuracy and limited interference. Among the optical techniques Infrared thermography (IR) is the most common method that has been used to measure microchannel wall temperatures. For example, Eain et al. [21] used an IR system to measure the local wall temperature along a stainless steel tube. They validated the accuracy of the results for each test by comparing them to the data that was obtained by thermocouples attached to the outer wall surface. This technique is based on measuring the spectra of infrared radiation that is emitted by an object to determine its temperature. Using this technique presents some challenges when measuring the wall temperature during an experiment, and prevents the use of insulation to reduce heat loss from the channel to the surroundings. It requires the exterior surface of the microchannel to be sprayed matt black, so as to increase the surface emissivity [21]. Minimizing radiation from high-temperature electrical instruments, lights, human bodies and the ambient surroundings are a difficult task in this system. Generally, calibration, measuring the surface emissivity and ambient radiation and measuring heat losses are the main challenges of the IR thermography system [22]. A detailed description of challenges in IR thermography is presented in [23].

The Wilson plot method [24] is another possible method that avoids the direct surface temperature measurement. The Wilson plot method along with its modified versions create a great tool for the analysis of convection heat transfer in tubes and heat exchangers for experimental research [25]. A detailed description of Wilson plot method is reviewed by Seara et al. [26].

Table 2 gives a summary of the temperature measurement methods in selected experimental investigations on the heat transfer of single-phase fluid flow in microchannels.

Table 2 Experimental studies on heat transfer of single-phase fluid flow in microchannels.

Authors	Geometry	Working fluids	Measurement techniques	Remarks
Peng et al. **[27]**	Rectangular Stainless steel	Water	TCs at inlet and outlet Six TCs on the outer surface	An error of 10 % was seen in the heat transfer coefficient 50<Re<4000 Nu was lower than the theoretical value for Re<100 Up to 30 % deviation in Nu calculation Eq. 5,6
Peng et al. **[27]**	Rectangular Stainless steel	Methanol	TCs at inlet and outlet Six TCs on the outer surface	An error of 10 % was seen in the heat transfer coefficient 700<Re<2000 Eq. 5,6
Harms et al. **[28]**	Rectangular Silicon	DI water	TCs at inlet and outlet	The uncertainties were not considered in the calculation An error of up to 0.5°C contributed to the error in *Nu* and its value was lower than the theoretical value.

				173<Re<3169 Eq.6
Qu et al. [6]	Single channel rectangular	DI water	TCs at inlet and outlet Four TCs inside the microchannel	Bulk Temperature increases linearly along the microchannel Excellent agreement between CFD and experiment. 139<Re<1672
Yen et al. [29]	Rectangular Stainless steel	-	TCs at inlet and outlet Twelve TCs glued with thermally conductive silicon to the outer wall	*Nu* number was lower than the theoretical value with the error greater than 10% in some points Eq. 5,6
Tiselj et al. [30]	Triangular Silicon	Water	TCs at inlet and outlet	Bulk water temperature and wall temperature do not change linearly along the channel 3.2<Re<64
Celata et al. [31]	Circular Glass tube		TCs at inlet and outlet Three TCs on the outer surface attached by non-conductive epoxy	Dependence of the Nusselt number on Re was observed 50<Re<2775 A deviation from theoretical value was seen for low Re.
Betz et al. [7]	Rectangular Aluminium	Water	TCs at inlet and outlet 15 TCs on the outer surface	4 % error in calculation *Nu* 100<Re<1500
Dasgupta et al.[17]	Circular Aluminium	DI water	RTDs at inlet and outlet	An error of 11 % was seen in the heat transfer coefficient 105<Re<159 Eq. 5,6
Liu at al. [32]	Circular and Rectangular Stainless steel	water	TCs at inlet and outlet Eight TCs on the outer surface	An error of 15% was seen in the heat transfer coefficient 2000<Re<10000
Szczukiewicz et al. [22]	Rectangular Silicon	R245fa	TCs at inlet and outlet Infra-red (IR) camera	Inlet and outlet TCs were located inside manifold's plenums A lower Nu was measured compared to the theoretical value with an error of 27.5 % 100 < Re < 1000 Eq. 5,6
Ho et al. [33]	Rectangular copper	Water-Al_2O_3	TCs at inlet and outlet Seven TCs embedded in holes close to the wall	Two plenums were used to make uniform temperature at inlet and outlet 133 < Re < 1515 Up to 16 % error in Nu Eq. 6

Dai et al. [9]	Rectangular Circular Aluminium	DI water	TCs at inlet and outlet 48 TCs on the outer surface	The conjugate heat transfer, entrance effects and temperature dependent viscosity variation and the cross-section geometry have significant effects on the heat transfer rate. For Re<250, a lower value of Nu was observed due to conjugate heat transfer. *Nu* was higher than the theoretical value for Re>500 due to the entrance effect. 50<Re<5000 Eq. 5,6
Rombault et al. [34]	Rectangular Aluminium	Cu-Water	TCs at inlet and outlet 12 TCs embedded in holes close to the wall	Microfabrication in needed to plant the TCs 100<Re<5000 Eq.5
Yu et al.[10]	Rectangular Pyrex	DI water-TiO_2	TFTs on the outer surface	An infrared camera was used for TC calibration. Good agreement between simulation and experiment results. The obtained *Nu* was significantly lower than the theoretical value. 1.7<Re<50
Zhang et al. [35]	Circular Stainless steel		TCs at inlet and outlet Eight TCs on the outer surface	The accuracy of inlet and outlet TCs is $\pm 1.5\ ^{0}C$ Averaged Inlet and the outlet temperature was used for calculating *Nu* 10% error in calculating *Nu* Eq.5
Sahar et al.[36]	Rectangular Copper	DI Water	TCs at inlet and outlet Eight TCs on the outer surface	Significant conjugate effects were seen It was difficult to measure local heat flux in microchannels 50 % error between CFD simulation and experiment. Eq.6 300<Re<3500
Kim [8]	Rectangular Aluminium	DI Water	RTDs at inlet and outlet 10 TCs embedded in holes close to the wall	Two plenums to ensure uniform inlet and outlet T For Re<180, the Nu was less than the theoretical value. For Re>180, the Nu was greater than the theoretical value. More than 15% error in calculating *Nu* Transferring heat from the test section to plenums affected the inlet T measurement. 30<Re<2500 Eq.6

3.2 Local fluid bulk temperature

Measuring the local bulk fluid temperature is required in order to calculate the local Nusselt number along the microchannel. There is a variety of direct and indirect techniques to measure the bulk fluid temperature.

Optical techniques can be used to directly measure the bulk fluid temperature. This technique is based on tracking a temperature sensitive dye which is added to the fluid. Laser Induced Fluorescence (LIF) and Molecular Tagging Thermometry (MTT) are the two common optical techniques to measure the temperature of fluid flow in microchannel flows [16]. However, due to their limitations, optical techniques are not commonly used for microchannels. The intensity of the applied light to the fluid flow and concentration of molecular dye have a significant effect on the accuracy of LIF temperature measurements. The applicability of MTT is questionable for microchannels having a small hydraulic diameter [16]. Additionally, in most of experimental studies, the microchannel is covered by insulation making it impossible to use these methods.

Planting thermocouples inside the microchannel is an alternative to directly measure the bulk fluid temperature, albeit at the cost of large disturbances in the flow through the microchannel. Additionally, this disturbance will be more significant with an increase in the number of the probes along the channel. Utilizing high accuracy fine thermocouples or micro RTDs can reduce the disturbance to the flow. As with the measurement of the wall temperature, the cost, complexities in fabrication and errors (due to the fluid flow being disturbed) are the limitations of this method, which has encouraged researchers to use indirect methods to measure the bulk fluid temperature.

Table 2 shows that indirect techniques are the most common method to calculate the bulk fluid temperature along the microchannel. In this technique, temperature probes are allocated just before and after the test section at the inlet and outlet, respectively. The bulk fluid temperature in the axial location can be calculated from an energy balance based on the inlet temperature as given by Eq.4. This is based on the assumption that a uniform heat flux is applied along the channel assuming that the C_p is constant for single phase fluid flow along the channel.

$$T_{b,x} = \frac{\Delta H}{C_p}\left(\frac{x}{L}\right) + T_{in} = \frac{\dot{Q}_{in}}{\dot{m}\, C_p}\left(\frac{x}{L}\right) + T_{in} \tag{4}$$

Predicting bulk temperature ($T_{b,x}$) along the test section (x) is dependent on the accuracy of inlet temperature measurement (T_{in}), the exact position of the measurement point, the accurate determination

of the mass flow rate ($\dot{m}$), heated length and the exact value of the heat flow through the microchannel walls ($\dot{Q}_{in}$). These effects are dominant in case of using two phase flow in microchannels. A discrepancy in measured position can increase the error in Nu. However, measuring the outlet temperature with a probe at the outlet can be helpful to validate the linear changes in bulk fluid temperature from the inlet to the outlet by comparing the measured temperature with that predicted by Eq. 4.

3.3 Input heat flux

In the experiment the total heat transfer rate is transferred to the fluid can be calculated by the two methods given in [20, 35, 37]:

$$\dot{\boldsymbol{Q}}_{\boldsymbol{in}} = \dot{\boldsymbol{Q}}_{\boldsymbol{e}} - \left(\frac{\boldsymbol{T}_{\boldsymbol{ave,w}} - \boldsymbol{T}_{\boldsymbol{a}}}{\boldsymbol{R}}\right) \tag{5}$$

$$\dot{Q}_{in} = \dot{m}\, C_p (T_{out} - T_{in}) \tag{6}$$

where $\dot{Q}_{in}$ and $\dot{Q}_e$ are the rate of heat in to the fluid and the electrical heat input, respectively. R is the equivalent thermal resistance for heat losses which can be determined through experimental calibration. The inlet (T_{in}) and outlet temperatures (T_{out}) can be measured with two thermocouples in the flow located before and after the test section. Both Eqn. 5 and 6 are applicable for experiments with single phase fluid flow. However, for experimental studies where it is not desirable to disturb the fluid flow, which is the case for two phase flow, Eq.6 is not an appropriate way to measure the input heat. Instead Eq.5 should be used to determine the value of the heat flux at the tube wall. In addition, it is hard to place the temperature probe in the exact position at the outlet and measure the accurate outlet temperature. In some studies [8, 33], the inlet and outlet temperatures were measured in plenums immediately before and after the test section. This may increase the error in measured inlet and outlet temperatures due to the conducted heat from the heated section to the manifolds. In experiments where two electrical connections are used to apply the Joule heating through the wall of the test section, the outlet temperature may differ from the true value as it is hard to place the thermocouple in the exact position at the inlet and outlet especially if there are unheated sections before and after the electrical connection points. In order to increase the accuracy of the measurement, performing an experiment for single phase flow using both Eq's. 5 and 6 allows the experimenter to estimate the accuracy of the measured heat loss and the measured input heat by comparing the results obtained from both equations In the case of electrical heating by Joule effect, the fluid needs to be dielectric and a special power source is required as the electrical current is generally high. Moreover, the high electrical current can result in energy loss in the conductors and terminals, and measurement of voltage in the test section is advised.

As discussed in section 3.1, the conjugate heat transfer effect is the most important parameter that may affect uniformity in heat flux along the microchannel. This parameter should be carefully considered in designing and calculation of heat transfer rate in microchannels.

3.4 Two-phase fluid flow

To date there have been many studies on convective single-phase heat transfer in microchannels, but recently there has been a growth in interest in heat transfer of two-phase flows in microchannels. A two-phase immiscible flow in a microchannel has a large potential to reduce the problems related to two-phase boiling flow in MCHSs, such as backflow and flow instability. Moreover, it has been found that two-phase flow can increases the Nusselt number for microchannel heat transfer by up to 400% over that for a single-phase fluid [5].

Performing experimental studies on two-phase flows have proved challenging as it requires the simultaneous control and measurement of many parameters. Although there have been numerous experimental researches on heat transfer of two-phase fluid flows in microchannels, confirming its increased rate of heat transfer over single-phase flow, there is a significant variation in the calculated heat transfer rates, particularly the *Nu* [5, 19, 38]. As it was mentioned in the previous sections, the possible sources of error could arise from the estimates of the wall temperature, the measured inlet temperature, the total heat transfer rate and the measurement of the bulk fluid temperature. In experimental studies of microscale two-phase fluid flow it is hard to accurately measure the bulk fluid temperature and the temperature at the inner surface of the wall. Locating probes at the inlet and outlet or close to inner walls disturb the fluid flow especially the film area (the region between a secondary phase and the solid wall) and can even burst the secondary phases [5]. This can affect the accuracy of the results obtained during the experiment. Therefore, most researchers have used an indirect method in their experiments to measure the wall temperatures and heat input through the fluid flow. In the case of Taylor flow of two immiscible liquids, the inlet temperature has been measured by averaging the temperature of the two phases measured just before they meet [39, 40]. This can be a source of error since the temperature can change between this point and the inlet of the test section. A temperature difference ranging from 0.01 to 0.3 ^{0}C in the inlet temperature measurement could result in an error of up to 20 percent in the calculation of the Nusselt number [19].

The accuracy of the measured position of probes at the wall is a key parameter to avoid errors in measuring the bulk fluid temperature of two-phase flow in the microchannels. A discrepancy of 2 mm in the measured position can give an error of 10 percent in calculating *Nu* [19]. In order to increase the accuracy of the measurement, performing a set of experiments for single phase flow prior to using two-phase flow can help validate the test rig measurement by comparing to the available data in the literature to the theoretical value for single-phase flow.

Application of optical methods in the measurement of temperatures in heat transfer study of single-phase flow in microchannels was discussed earlier. In most of the experimental studies, it is hard to visualize the fluid flow inside the test section as it is covered by insulation and the walls of the test section are typically opaque. However, Asthana et al. [41] did experimental study on the heat transfer of water-mineral oil in a microchannel with a quartz mask on top of the test section. Laser-induced fluorescence (LIF) was used to obtain the fluid temperature. However, an error of more than 30 percent was seen in their results. This indicates the difficulties in finding the accurate wall and bulk fluid temperature in two-phase flow in the microchannels with LIF. Moreover, the light from the visualization system could possibly affect the wall temperature readings by RTDs and add an extra source of heating to the fluid [42].

It is important to run the two-phase fluid flow experiment in a range of Reynolds numbers for which the test rig had been validated for single-phase flow. This is essential as a deviation from theoretical value has been seen for *Nu* especially in low and high Reynolds number [10, 41]. Therefore, considering the non-dimensional groups mentioned in Table 1, it is vital before designing any experimental test rig to eliminate or consider the scaling effects or errors in the calculation of the Nusselt number.

Table 3 summarises temperature measurement methods used in selected experimental studies of heat transfer of two-phase fluid flow in microchannels. Among studies that have been conducted on two-phase flow regimes, the indirect method has been the most common method used to obtain the wall and bulk fluid temperatures. In some cases, it was not possible to locate temperature probes at the inlet or outlet of the test section due to the presence of a visualization section after or before the test section. In these cases the applied heat flux was determined using Eq.5.

Table 3 Experimental studies of heat transfer of Two-phase fluid flow in microchannels.

Authors	Geometry	Working fluids	Measurement techniques	Remarks
Yen et al. **[29]**	Circular Stainless steel	HCFC123 FC72	TCs at inlet and outlet Twelve TCs glued to the outer wall	The accuracy of Measured heat transfer coefficient was ±10%. 20<Re<265 The error in the Nu estimation for boiling two-phase flow was lower than for single-phase flow. Eq.5,6
Agarwal et al.**[18]**	barrel-shaped, N-shaped, rectangular, square, and triangular	R134a	RTDs on the wall	High uncertainty for the low mass flux due to the difficulty of temperature measurement Eq.5
Betz et al. **[7]**	Rectangular Aluminium	Water-Air	TCs at inlet and outlet 15 TCs on the outer surface	4 % error in calculation *Nu* 100<Re<1500
Asthana et al. **[41]**	Rectangular Silicon	Water-light mineral oil	LIF	An error of more than 30 % was found the in calculated *Nu*

				6<Re<9
Liu et al. [43]	Rectangular Silicon	Methanol, Helium	TCs at inlet and outlet	An error up to 15 % was found in results Eq.6
Alam et al. [44]	Rectangular silicon	Boiling two-phase flow (DI water)	TCs at inlet and outlet	An error of 4-10% was found Eq.6
Al-Hajri et al.[45]	Rectangular	R-134a R-245fa	TCs at inlet and outlet Five TCs on the wall	An error of 11 % was seen in the heat transfer coefficients Eq.5
Liu at al. [32]	Circular Rectangular Stainless steel	Water-R152a	TCs at inlet and outlet Eight TCs on the outer surface	An error 30% was seen in the heat transfer coefficients 2000<Re<10000
Houshmand et al. [42]	Rectangular Copper and Pyrex	Water- Air	RTDs on the wall	The light from the visualization system could affect the RTDs Eq.5
Giolla Eain et al. [21]	Circular Stainless steel	Oils-water	IR thermography for measuring wall and inlet T	10-30 % error in calculating *Nu* 2.3<Re<92.1
Dai et al. [19]	Circular Stainless steel	Oils-water	Six RTDs on the outer surface	Error up to 45% in calculating *Nu* which was highly dependent on the inlet temperature accuracy.
Zhang et al. [35]	Circular Stainless steel		TCs at inlet and outlet Eight TCs on the outer surface	The accuracy of inlet and outlet TC was $\pm$ 1.5 ^{0}C Averaged Inlet and the outlet temperature was used for *Nu* Eq.5

4 Experimental study

An experimental study of heat transfer to a single phase fluid in a square test section has been conducted in order to illustrate the propagation of errors in the estimation of the Nusselt number, and the effects of some dimensionless groups. Fig.1 shows the microchannel experimental apparatus which was designed for single phase and two-phase (immiscible phases) fluid flow. Each of the two phases was passed through an acrylic T-junction with a dedicated flow controller (Alicat_LC10CCM) in each line. The test section was made of a single channel of stainless steel 304 (produced by Changsha Jetsun Trade Development Co., Ltd , China) with a square cross-section of 2mm × 2mm, wall thickness 0.5 mm, and length 300 mm. The heating section was covered by insulation (RS.Pro-superwool 607,$k = 0.05\ W/m.k$) to reduce heat losses to the surroundings. The stainless steel tube was placed between two acrylic tubes

with length of 300mm, with the same inner cross section, located at both ends for flow visualization. The acrylic tubes are beneficial to minimize the heat loss at the ends as they have a low thermal conductivity and ensured that a hydrodynamic fully developed flow entered the microchannel as the entrance length (L_e)in this study is less than 300 mm ($\frac{L_e}{D} \approx 0.06\ Re$) . The tube was connected to the acrylic sections by a high temperature silicon gasket. A total of eighteen T-type thermocouples were soldered to the top and bottom outer surface of the test section, and two thermocouples were located within the fluid channels immediately before the T junction where the two phases meet ($T_{i,1}\ and\ T_{i,2}$). A T-type thermocouple ($T_{i,3}$) was place precisely just before the heating tube entrance covered with an ultra-thin layer of acrylic cement so as not to disturb the fluid flow. This is particularly important for experiments with two phase flow. Two fine holes (0.5 mm diameter) were placed just before and after the tube to place two thermocouples ($T_{i,4}\ and\ T_o$) in contact with the fluid directly to measure the inlet (T4) and outlet temperature. These temperature probes are for calibration and were able to be removed when required. The T-type thermocouples are in-house made from 0.2 mm diameter copper and constantan wire (Concordia Wire and Cable Co. Ltd). The room air temperature was measured using a K-type thermometer (DSE-Q1437). All the thermocouples were carefully calibrated in a water bath (Julabo-MD-BRU/PU) at atmospheric pressure and to an accuracy of ± 0.05 °C using a digital thermometer (Ebro TFX 430 with ± 0.019 resolution). Temperature data was collected by a data acquisition system (National instruments-cRIO-9063). The constant heat flux was applied via Joule heating of the stainless steel test section, from an electrical power supplied (2001 Function generator and high power stereo amplifier Citronic-AEL600) using two clamps attached to the ends of the test section with a spacing of 296 mm. The current and voltage supplied to the test section were measured by two digital multifunction instruments (TENMA- 726185 and KEITHLEY-195A). Distilled water was used as the working fluid.

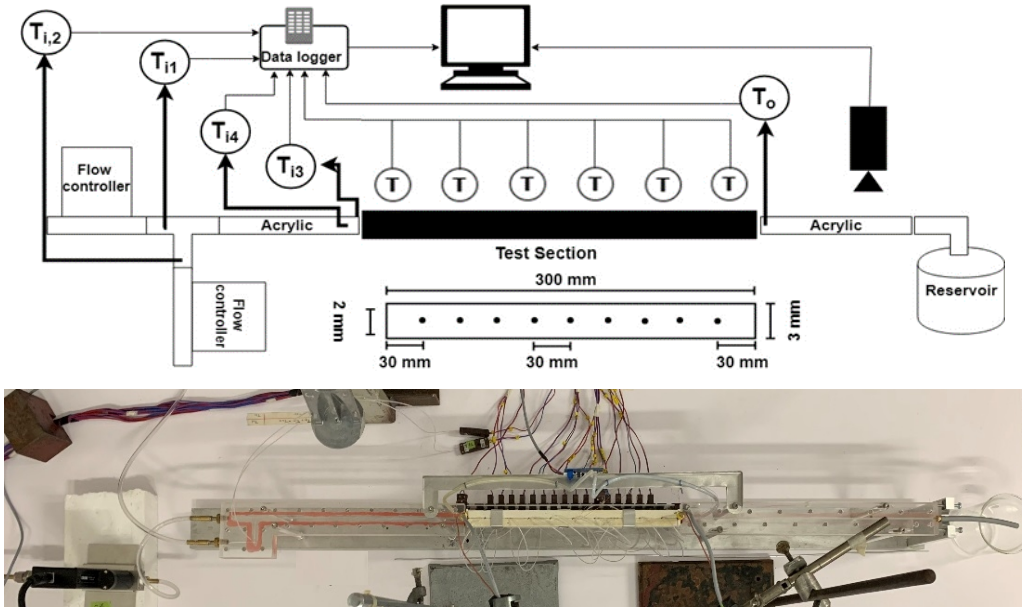

Fig. 1 Schematic and photograph of the experimental rig

To estimate the heat losses, power was applied to the test section with no fluid flow. The potential heat losses will be free convection, conduction, and radiation. As there is no working fluid involved, the total heat input is equal to heat losses, $\dot{Q}_e = VI = \dot{Q}_{loss} = \frac{1}{R}(T_{ave,w} - T_a)$. The average wall temperature $T_{ave,w}$ was measured by averaging all the thermocouples attached to the tube. A second-order polynomial fit was used to find the heat loss coefficient trend from Fig.2 as follows:

$$\boldsymbol{C = \frac{1}{R} = -1 \times 10^{-5}(T_{ave,w} - T_a)^2 + 5 \times 10^{-5}(T_{ave,w} - T_a) + 0.0538} \quad (7)$$

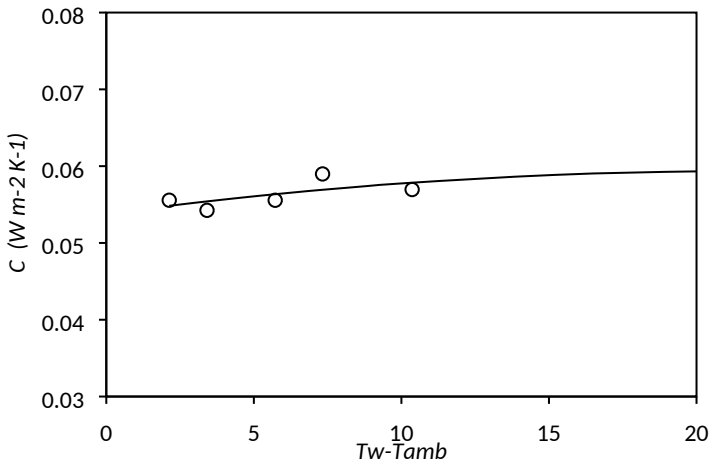

Fig. 2 Heat loss coefficient for the test section

A series of experiments for single-phase water flow was conducted in the microchannel to measure the heat transfer rate. Flow rates ranging from 2 to 10 ml/min (corresponding to a Reynolds number of $18 < Re < 95$) were used. The power supply, and therefore the heat input, was varied by adjusting the voltage. The data was collected for a period of 60 s after 2000 seconds when the test section had reached

steady state (Fig.3) and averaged. Each test was repeated three times in order to obtain a set of reliable data, and confirm repeatability.

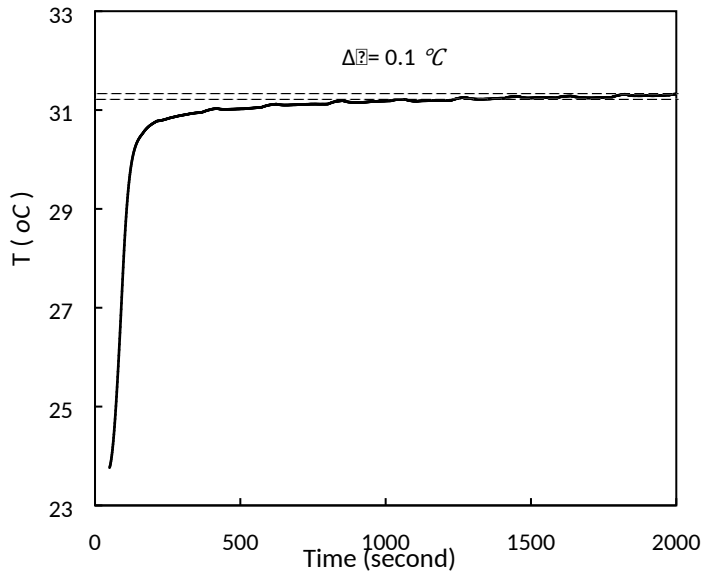

Fig. 3 Steady state condition

Table 4 shows a summary of the accuracy of the measurements in the current experiment. The uncertainties were estimated based on the standard approach proposed by Moffat et al. [46]. The inaccuracy at the inlet temperature measurement and inlet flow rate are the major source of error as the bulk fluid temperature was calculated by Eq.4 based on the directly measured inlet temperature. An error ranging from ±0.1℃ to ±0.5℃ in the inlet temperature measurement was found to increase the error in Nusselt number by up to 20 percent. However, in this study the inlet temperature accuracy is ±0.05℃ due to careful calibration. At low Reynolds numbers, an error of ±0.2 ml/min in the inlet flow rate can increase the error in the Nusselt number by up to 40 per cent. Thus, aside from the flow controller, a high precision scale (METTLER TOLEDO-AG204) was used to determine the flow rate for each test as the accuracy of inlet flow rate affects the bulk fluid temperature measurement. Another source of error is the quantification of the rate of heat flux applied to the test section. However, inaccuracy of applied heat in most of the cases was found to be less than 5 percent and this has a minor effect on the Nusselt number calculation. The experiments were carried out over the temperature range of 25 ℃ to 45℃, and the corresponding variation in fluid properties had only a minor effect (less than 2 %) on the calculated average Nusselt number.

Table 4 Maximum measurement uncertainties

variable	Accuracy
Volumetric flow rate	$<\pm$ 0.05 (ml/min)
Electrical voltage	$\pm$ 0.0005 (V)

Electrical current	± 0.01 (*A*)
Thermocouples	± 0.05 (℃)
Heat flux	<± 5 (%)
Nusselt number	< ± 5 (%)

4.1 CFD simulation

In order to study the three-dimensional heat transfer characteristics in the test section, a series of simulations were run using ANSYS Fluent v17 modelling the geometry of the experimental rig including the test section, insulation, acrylic tubes and the two clamps at the ends of the stainless steel tube. As the fluid flow in the square test section was symmetric, a quarter of the test section was simulated by using two symmetry planes in the *xz* and *yz* planes, as shown in Fig.4. A range of *Re* from 18 to 100 was modelled to allow direct comparison between CFD and experiment. This range of *Re* is chosen as inaccuracy in Nusselt number calculation increases at low *Re*. This will be discussed in detail in section 4.2.3.

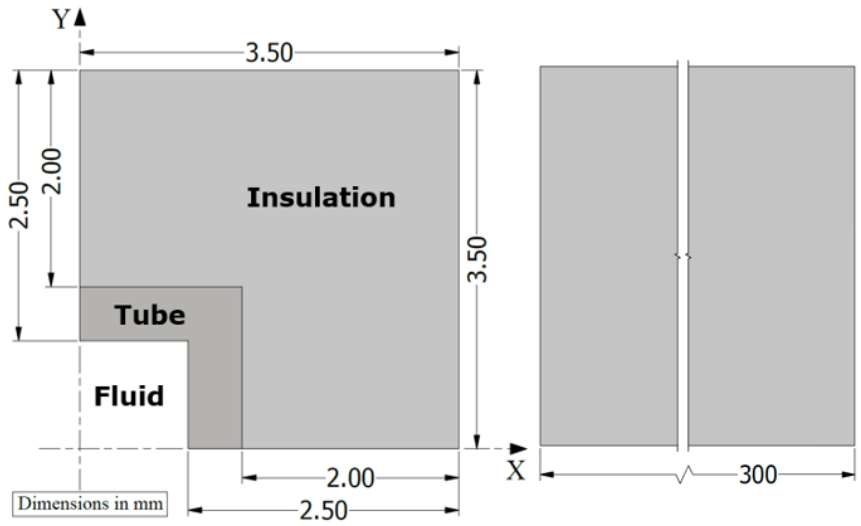

Fig. 4 The computational domain for the conjugate convection and conduction simulations.

The continuity, momentum and energy equations were solved for laminar flow and heat transfer in the microchannel, using the following assumptions and boundary conditions;

- the fluid in the channel was incompressible and Newtonian.
- there was no viscous dissipation.
- fluid properties were independent of temperature.
- no-slip boundary conditions on the walls.
- fully developed velocity profile prescribed at the inlet.

- zero velocity and temperature gradient at the outlet and prescribed pressure.
- constant heat source within the test section wall calculated from the experiment

The numerical computations were performed by solving the governing equations (continuity, momentum and energy equations) along with the boundary conditions using the finite volume method (FVM). The SIMPLE algorithm was used, and the momentum and energy equations were discretised using a second order upwind difference scheme. The convergence criterion was set to 10^{-8} for all variables.

A grid dependency test was performed for the water flow in the geometry to make sure the mesh size had a minimal effect on the solution. Three meshes denoted coarse, medium and fine, were tested, containing 5.4×10^5 1.08×10^6 and 2.3×10^6 nodes respectively. The Nusselt numbers for the three meshes were compared, and it was determined by changing the mesh size from medium to fine, that the Nusselt number varies by only 1 %. To reduce the computation time, the medium mesh of 1.08×10^6 nodes was selected for further simulations.

4.2 Results and discussion

4.2.1 Inlet temperature measurement

The accuracy of the inlet temperature measurement has a significant effect on the accuracy of the predicted bulk fluid temperature along the test section. For single phase flow the inlet temperature was measured for different flow rates with $T_{i,1}$, $T_{i,3}$ and $T_{i,4}$ (refer to Fig. 1; thermocouple 1 is located before the T section, while thermocouples 3 and 4 are at the test section inlet, with 3 being immersed in the flow and 4 being located at the wall inner surface). There was no major difference between the measured inlet temperatures $T_{i,3}$ and $T_{i,4}$, with the difference between them being less than 0.08℃. Moreover, the inlet temperature for the lowest flow rate at this point was constant during the test, confirming that the heated test section does not affect the inlet temperature. The same behaviour was observed in the CFD simulation. However, in the experiment a temperature difference of up to 0.5℃ was seen between $T_{i,1}$, $and\ T_{i,3}$. This could be a source of error in calculating the Nusselt number. It is worth noting that in some the experimental studies with two phase fluid flow [19, 35], the inlet temperature was measured far from the inlet due to the limitations discussed in section 3.4, and this could have been a major source of error in these experiments. Therefore in this study the temperature measured by $T_{i,3}$ was used in the rest of calculations.

4.2.2 Total applied heat flow

The total rate of heat that was transferred to the fluid flow was calculated using Eq's. 5 and 6. Fig.5 shows the input heat to the test section determined by Eq.5 compared to the increase in the enthalpy of the flow calculated with Eq.6. In most cases the difference between the two values was less than 5 percent. There is one case, at *Re*=18, with an error of 10.7%. However, overall there is a good agreement

between both methods used to determine the rate that heat was transferred to the fluid flow. Moreover, this can validate the calculation of input heat using Eq. 5. Generally, the total heat loss to the ambient was in the range of 5 to 16% of the electrical energy applied to the wall. This means that the bulk of the power input is transferred to the working fluid, but the heat losses to the surrounds are non-negligible.

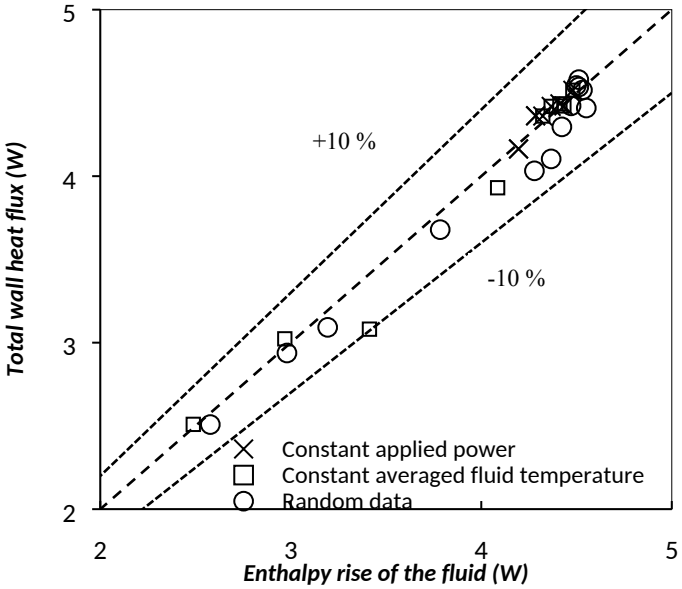

Fig. 5 Comparison of the estimated total wall heat flux with the enthalpy rise of the fluid flow

Fig.6 shows that there is good agreement between the measured outlet temperature and that predicted by Eq. 4, as might be expected from the data shown in Fig.5. This confirms the applicability of using Eq.4 to determine the bulk temperature along the heated test section. Fig.7a-b depict the local wall temperature and the local bulk fluid temperature with axial position along the heated test section for two Reynolds numbers with constant applied heat flux. Both experimental and CFD data are presented. The experimental inner wall temperature was calculated from the outer wall temperature measurements by means of a one-dimensional heat conduction analysis. However, the temperature difference in the current study was found to be negligible, with errors of less than 0.01℃. As it was expected, given the heat flux was uniform along the test section, the wall and bulk fluid temperature increased linearly along the wall and the temperature difference between the wall and bulk fluid remains constant. The general trend of the temperature measurements shows that a uniform constant heat flux is applied to the test section. It can be seen that the CFD results for wall and bulk fluid temperature are matched with the experiment. However, there is a slight difference in the wall temperature at the exit of the test section. This is due to the heat loss at the ends of the tube and this deviation is decreased by increasing the Reynolds number. To minimize the entrance effect and possible dicrepancies at the end of the channel, the first and last thermocouples data are henceforth not considered in the determination of the Nusselt number.

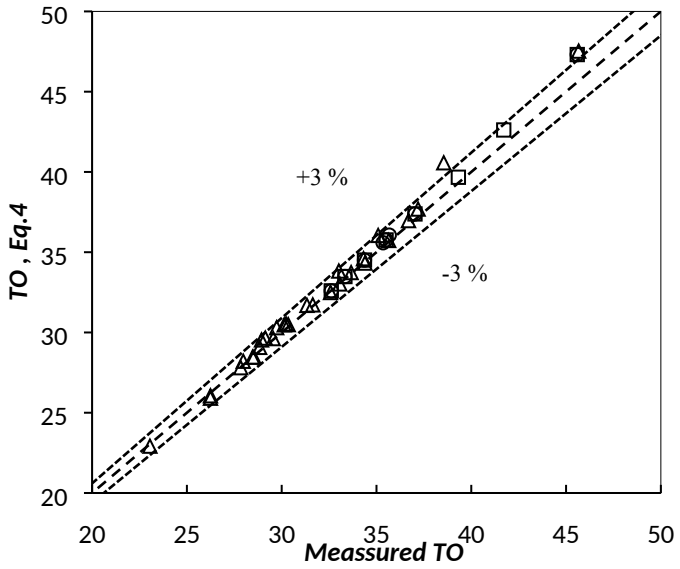

Fig. 6 Comparison of predicted and measured outlet temperature (°C)

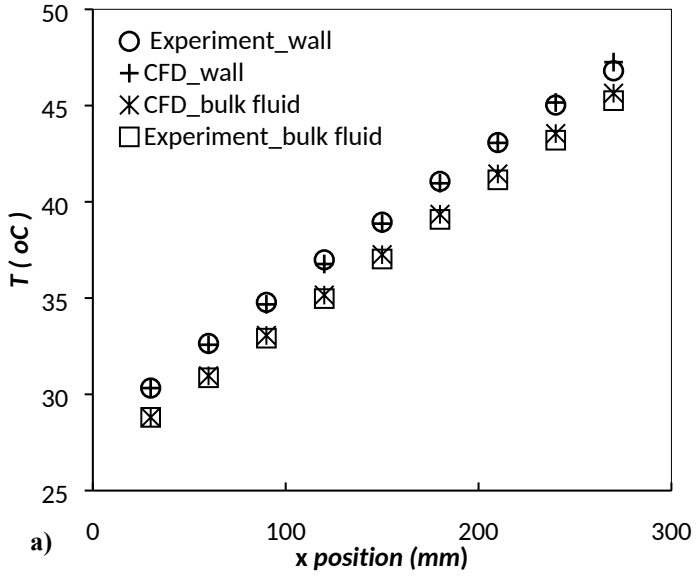

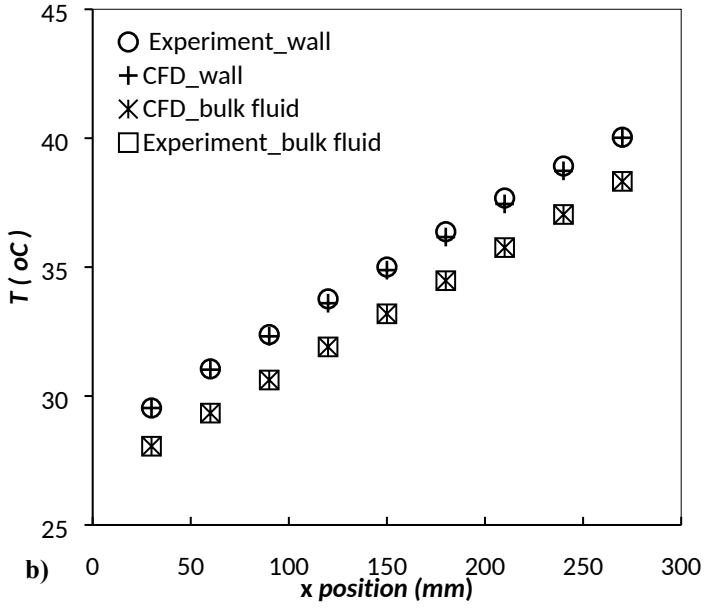

Fig. 7 Comparison of experimental and CFD wall and bulk fluid temperatures at $\dot{Q}_{in} = 4.5\ W$ for a) *Re*=28 and b) *Re*=45

4.2.3 Nusselt number

For low values of Reynolds number, the entrance length is very short and the viscous dissipation effects are not significant. However, for low Reynolds number the conjugate heat transfer effects on Nusselt number could be large in comparison with convection [14]. In this study, the value of *M* remains below the limit given in Table 1 ($M < 10^{-4}$) to reduce the effect of axial wall conduction. Fig.8-a shows the averaged Nusselt number in the test section, versus the Reynolds number which is determined from the flow rate set by the flow controller. It can be seen that the Nusselt number depends on the Reynolds number, although this dependency decreases with increasing Reynolds number. This same trend has been reported by many researchers as stated in Table 2. The averaged Nusselt number was calculated by averaging the local Nusselt number in the locations where its value became constant. For Reynolds numbers greater than 45, the measured Nusselt numbers are close to the theoretical value of 3.09. However, the Nusselt numbers are underestimated for Reynolds numbers less than 40 with an error of 15 to 40 per cent. This could possibly be due to the unforeseen parameters that had an effect similar to axial wall conduction [8, 31, 47]. However, as it was discussed earlier, the accuracy of the calculation of the Nusselt number is highly dependent on the accuracy of the wall and bulk fluid temperature measurements. As the indirect method was used to predict the bulk fluid temperature, any small error could result in errors in the calculated Nusselt number.

The accuracy of inlet flow rate is a key parameter when using the indirect method to measure the bulk fluid temperature. To examine the influence of errors in flow rate measurement, a precession scale was used to measure the flow rate precisely while the flow controller was running to provide a uniform inlet flow rate. An error of 0.1-0.2 g/min was found in the inlet flow rate measurement, which resulted in an error of up to 40% in the calculation of the Nusselt number. This error decreases with increasing Reynolds number. Fig.8-b presents a second set of Nusselt numbers obtained after measuring the inlet flow rate more precisely. The calculated Nusselt number is now independent of Reynolds number for Re > 20 and it is in an agreement with the theoretical value (3.09) given by Shah et al. [48] with an error of less than 10 per cent. For a Reynolds number of 18, the difference from the theoretical value is approximately 15 per cent, possibly due to a large heat loss at the ends of the test section although further study is needed to determine this.

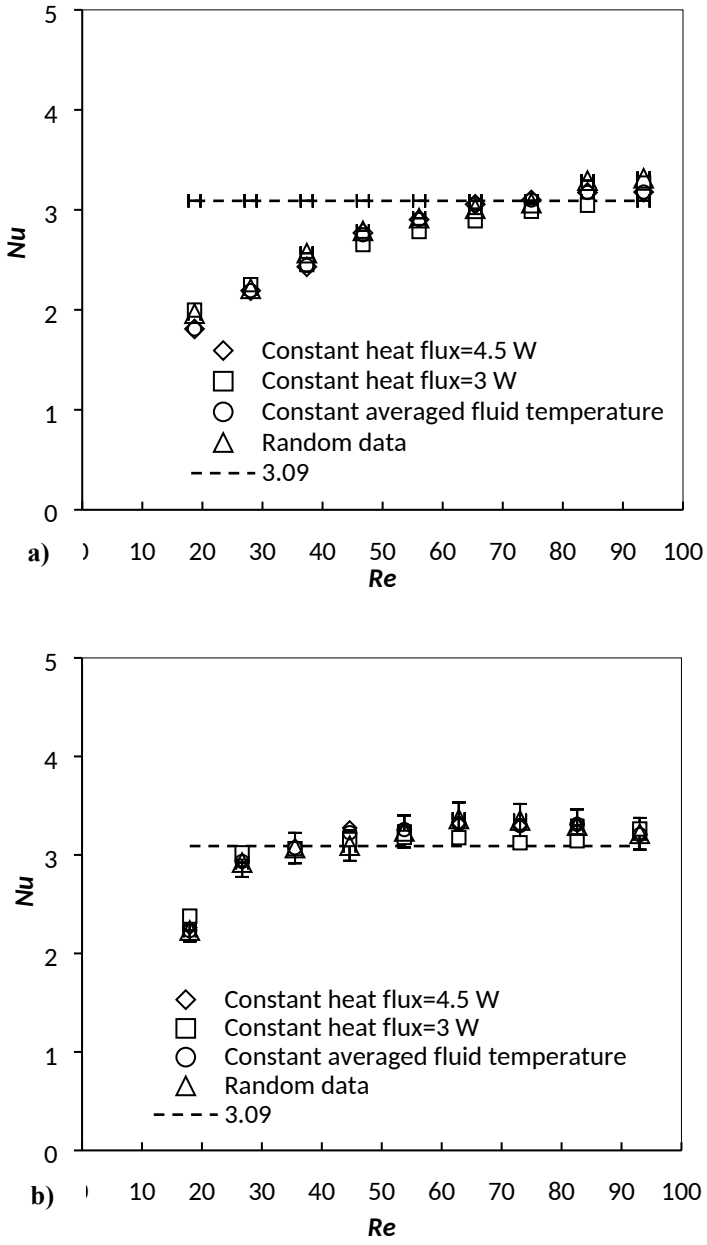

Fig. 8 Comparison of experimental measurements and analytic prediction of average Nusselt number for 20 < Re < 95, (a) using mass flow rates measured by the flow controller, and (b) using mass flows rates measured using a balance and stopwatch.

5 Conclusions

This paper has reviewed experimental studies of single and two-phase fluid flow heat transfer in microchannels. A complete summary of the heat transfer measurement methods and important parameters affecting the accuracy of the temperature measurements has been presented. The indirect method was the most common technique to measure the inner wall temperatures and the bulk fluid temperature. The effect of conjugate heat transfer in the channel walls, entrance length and viscous dissipation are parameters that dominate the accuracy of indirect methods of temperature measurement, while error in the measurement of the inlet flow rate significantly affects the accuracy of heat transfer measurements at low Reynolds numbers. Performing a CFD simulation of the combined channel and

wall geometry can be beneficial to quantify errors and ensure all the assumptions made in the processing of the experimental data are valid.

The experimental data that has been presented demonstrates that without considering these effects, deriving a correlation to predict *Nu* is not reliable. Based on the experimental data from the present study, the classical theory of heat transfer is reliable for microchannels for Reynolds numbers as low as 20. This is in contrast to the literature which claims that the Nusselt number decreases significantly when the Reynolds number is reduced from 100 to 20. This is most likely due to the sources of experimental error that have been demonstrated in the present study. Further study is recommended at lower Reynolds numbers.

References

[1] P. Smakulski, S. Pietrowicz, A review of the capabilities of high heat flux removal by porous materials, microchannels and spray cooling techniques, Applied Thermal Engineering, 104 (2016) 636-646.
[2] L. Chai, G. Xia, M. Zhou, J. Li, J. Qi, Optimum thermal design of interrupted microchannel heat sink with rectangular ribs in the transverse microchambers, Applied Thermal Engineering, 51(1-2) (2013) 880-889.
[3] D.B. Tuckerman, R.F.W. Pease, High-Performance Heat Sinking for VLSI, IEEE Electron Device Letters, EDL-2(5) (1981) 126-129.
[4] W. Qu, I. Mudawar, Prediction and measurement of incipient boiling heat flux in micro-channel heat sinks, International Journal of Heat and Mass Transfer, 45(19) (2002) 3933-3945.
[5] A. Abdollahi, R.N. Sharma, A. Vatani, Fluid flow and heat transfer of liquid-liquid two phase flow in microchannels: A review, International Communications in Heat and Mass Transfer, 84 (2017) 66-74.
[6] W. Qu, I. Mudawar, Experimental and numerical study of pressure drop and heat transfer in a single-phase micro-channel heat sink, International Journal of Heat and Mass Transfer, 45(12) (2002) 2549-2565.
[7] A.R. Betz, D. Attinger, Can segmented flow enhance heat transfer in microchannel heat sinks?, International Journal of Heat and Mass Transfer, 53(19-20) (2010) 3683-3691.
[8] B. Kim, An experimental study on fully developed laminar flow and heat transfer in rectangular microchannels, International Journal of Heat and Fluid Flow, 62 (2016) 224-232.
[9] B. Dai, M. Li, C. Dang, Y. Ma, Q. Chen, Investigation on convective heat transfer characteristics of single phase liquid flow in multi-port micro-channel tubes, International Journal of Heat and Mass Transfer, 70 (2014) 114-118.
[10] J. Yu, S.-W. Kang, R.-G. Jeong, D. Banerjee, Experimental validation of numerical predictions for forced convective heat transfer of nanofluids in a microchannel, International Journal of Heat and Fluid Flow, 62 (2016) 203-212.
[11] M. Asadi, G. Xie, B. Sunden, A review of heat transfer and pressure drop characteristics of single and two-phase microchannels, International Journal of Heat and Mass Transfer, 79 (2014) 34-53.
[12] G.L. Morini, Y. Yang, Guidelines for the Determination of Single-Phase Forced Convection Coefficients in Microchannels, Journal of Heat Transfer, 135(10) (2013) 101004-101004-101010.
[13] L.P. Yarin, A. Mosyak, G. Hetsroni, Heat Transfer in Single-Phase Flows, in: Fluid Flow, Heat Transfer and Boiling in Micro-Channels, Springer Berlin Heidelberg, Berlin, Heidelberg, 2009, pp. 145-194.
[14] P. Rosa, T.G. Karayiannis, M.W. Collins, Single-phase heat transfer in microchannels: The importance of scaling effects, Applied Thermal Engineering, 29(17) (2009) 3447-3468.

[15] G.L. Morini, Y. Yang, H. Chalabi, M. Lorenzini, A critical review of the measurement techniques for the analysis of gas microflows through microchannels, Experimental Thermal and Fluid Science, 35(6) (2011) 849-865.
[16] G.L. Morini, The Challenge to Measure Single-phase Convective Heat Transfer Coefficients in Microchannels, Heat Transfer Engineering, (2018) 1-16.
[17] E.S. Dasgupta, S. Askar, M. Ismail, A. Fartaj, M.A. Quaiyum, Air cooling by multiport slabs heat exchanger: An experimental approach, Experimental Thermal and Fluid Science, 42 (2012) 46-54.
[18] A. Agarwal, T.M. Bandhauer, S. Garimella, Measurement and modeling of condensation heat transfer in non-circular microchannels, International Journal of Refrigeration, 33(6) (2010) 1169-1179.
[19] Z. Dai, Z. Guo, D.F. Fletcher, B.S. Haynes, Taylor flow heat transfer in microchannels—Unification of liquid–liquid and gas–liquid results, Chemical Engineering Science, 138 (2015) 140-152.
[20] T.-H. Yen, N. Kasagi, Y. Suzuki, Forced convective boiling heat transfer in microtubes at low mass and heat fluxes, International Journal of Multiphase Flow, 29(12) (2003) 1771-1792.
[21] M. Mac Giolla Eain, V. Egan, J. Punch, Local Nusselt number enhancements in liquid–liquid Taylor flows, International Journal of Heat and Mass Transfer, 80 (2015) 85-97.
[22] S. Szczukiewicz, N. Borhani, J.R. Thome, Fine-resolution two-phase flow heat transfer coefficient measurements of refrigerants in multi-microchannel evaporators, International Journal of Heat and Mass Transfer, 67 (2013) 913-929.
[23] T. Astarita, G. Cardone, G.M. Carlomagno, C. Meola, A survey on infrared thermography for convective heat transfer measurements, Optics & Laser Technology, 32(7) (2000) 593-610.
[24] E.E. Wilson, A Basis for Rational Design of Heat Transfer Apparatus, The J. Am. Soc. Mech. Engrs., 37 (1915) 546-551.
[25] J. Fernández-Seara, F.J. Uhía, J. Sieres, Laboratory Practices with the Wilson Plot Method, Experimental Heat Transfer, 20(2) (2007) 123-135.
[26] J. Fernández-Seara, F.J. Uhía, J. Sieres, A. Campo, A general review of the Wilson plot method and its modifications to determine convection coefficients in heat exchange devices, Applied Thermal Engineering, 27(17) (2007) 2745-2757.
[27] X.F. Peng, G.P. Peterson, Convective heat transfer and flow friction for water flow in microchannel structures, International Journal of Heat and Mass Transfer, 39(12) (1996) 2599-2608.
[28] T.M. Harms, M.J. Kazmierczak, F.M. Gerner, Developing convective heat transfer in deep rectangular microchannels, International Journal of Heat and Fluid Flow, 20(2) (1999) 149-157.
[29] T.H. Yen, N. Kasagi, Y. Suzuki, Forced convective boiling heat transfer in microtubes at low mass and heat fluxes, International Journal of Multiphase Flow, 29(12) (2003) 1771-1792.
[30] I. Tiselj, G. Hetsroni, B. Mavko, A. Mosyak, E. Pogrebnyak, Z. Segal, Effect of axial conduction on the heat transfer in micro-channels, International Journal of Heat and Mass Transfer, 47(12–13) (2004) 2551-2565.
[31] G.P. Celata, M. Cumo, V. Marconi, S.J. McPhail, G. Zummo, Microtube liquid single-phase heat transfer in laminar flow, International Journal of Heat and Mass Transfer, 49(19) (2006) 3538-3546.
[32] N. Liu, J.M. Li, J. Sun, H.S. Wang, Heat transfer and pressure drop during condensation of R152a in circular and square microchannels, Experimental Thermal and Fluid Science, 47 (2013) 60-67.
[33] C.J. Ho, W.C. Chen, An experimental study on thermal performance of Al2O3/water nanofluid in a minichannel heat sink, Applied Thermal Engineering, 50(1) (2013) 516-522.
[34] B. Rimbault, C.T. Nguyen, N. Galanis, Experimental investigation of CuO–water nanofluid flow and heat transfer inside a microchannel heat sink, International Journal of Thermal Sciences, 84 (2014) 275-292.
[35] B. Zhang, Y. Wang, J. Zhang, Q. Li, Experimental research on pressure drop fluctuation of two-phase flow in single horizontal mini-channels, Experimental Thermal and Fluid Science, 88 (2017) 160-170.
[36] A.M. Sahar, M.R. Özdemir, E.M. Fayyadh, J. Wissink, M.M. Mahmoud, T.G. Karayiannis, Single phase flow pressure drop and heat transfer in rectangular metallic microchannels, Applied Thermal Engineering, 93 (2016) 1324-1336.

[37] T. Layssac, S. Lips, R. Revellin, Effect of inclination on heat transfer coefficient during flow boiling in a mini-channel, International Journal of Heat and Mass Transfer, 132 (2019) 508-518.
[38] T. Bandara, N.-T. Nguyen, G. Rosengarten, Slug flow heat transfer without phase change in microchannels: A review, Chemical Engineering Science, 126 (2015) 283-295.
[39] S.S.Y. Leung, Y. Liu, D.F. Fletcher, B.S. Haynes, Heat transfer in well-characterised Taylor flow, Chemical Engineering Science, 65(24) (2010) 6379-6388.
[40] S.S.Y. Leung, R. Gupta, D.F. Fletcher, B.S. Haynes, Effect of flow characteristics on Taylor flow heat transfer, Industrial and Engineering Chemistry Research, 51(4) (2012) 2010-2020.
[41] A. Asthana, I. Zinovik, C. Weinmueller, D. Poulikakos, Significant Nusselt number increase in microchannels with a segmented flow of two immiscible liquids: An experimental study, International Journal of Heat and Mass Transfer, 54(7-8) (2011) 1456-1464.
[42] F. Houshmand, Y. Peles, Heat transfer enhancement with liquid–gas flow in microchannels and the effect of thermal boundary layer, International Journal of Heat and Mass Transfer, 70 (2014) 725-733.
[43] T.L. Liu, B.R. Fu, C. Pan, Boiling heat transfer of co- and counter-current microchannel heat exchangers with gas heating, International Journal of Heat and Mass Transfer, 56(1-2) (2013) 20-29.
[44] T. Alam, P.S. Lee, C.R. Yap, L. Jin, A comparative study of flow boiling heat transfer and pressure drop characteristics in microgap and microchannel heat sink and an evaluation of microgap heat sink for hotspot mitigation, International Journal of Heat and Mass Transfer, 58(1-2) (2013) 335-347.
[45] E. Al-Hajri, A.H. Shooshtari, S. Dessiatoun, M.M. Ohadi, Performance characterization of R134a and R245fa in a high aspect ratio microchannel condenser, International Journal of Refrigeration, 36(2) (2013) 588-600.
[46] R.J. Moffat, Describing the uncertainties in experimental results, Experimental Thermal and Fluid Science, 1(1) (1988) 3-17.
[47] G.L. Morini, Scaling Effects for Liquid Flows in Microchannels, Heat Transfer Engineering, 27(4) (2006) 64-73.
[48] R.K. Shah, A.L. London, Chapter VII - Rectangular Ducts, in: R.K. Shah, A.L. London (Eds.) Laminar Flow Forced Convection in Ducts, Academic Press, 1978, pp. 196-222.